On π-line reconstruction formulas in tomography

Adel Faridani

Joint work with **Ryan Hass**

Department of Mathematics

Oregon State University

faridani@math.oregonstate.edu

http://people.oregonstate.edu/ faridana/

January 14, 2014

Tomography with sources on a curve

Data: Measurements of the divergent beam transform

$$\mathcal{D}f(\mathbf{y}, \boldsymbol{\theta}) = \int_0^\infty f(\mathbf{y} + t\boldsymbol{\theta})\, dt.$$

$$\mathbf{y}(s) \;=\; \text{source curve.}$$

Example 1: 2D fan-beam tomography

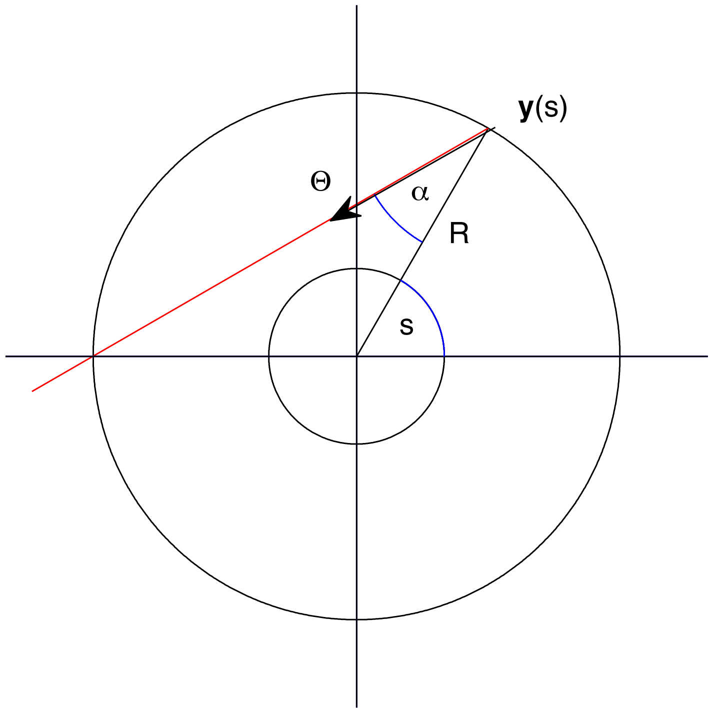

$$\mathbf{y}(s) = R(\cos(s), \sin(s)), \quad Df(\mathbf{y}(s), \mathbf{\Theta}(s,\alpha)) = g(s,\alpha)$$

$(s, \alpha) =$ "curved detector coordinates".

Example 2: 3D Helical Tomography

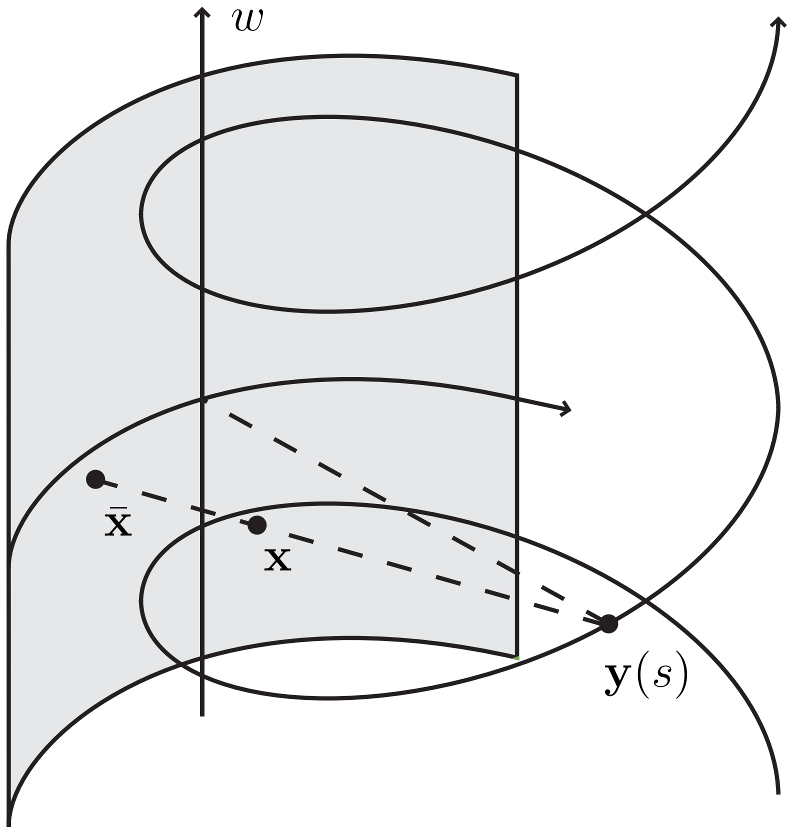

Source Curve: $\mathbf{y}(s) = \left[R\cos(s),\ R\sin(s),\ \frac{P}{2\pi}s \right]$

Let S denote the interior of the helix cylinder. supp$(f) \subset S$.

Example 2: 3D Helical Tomography

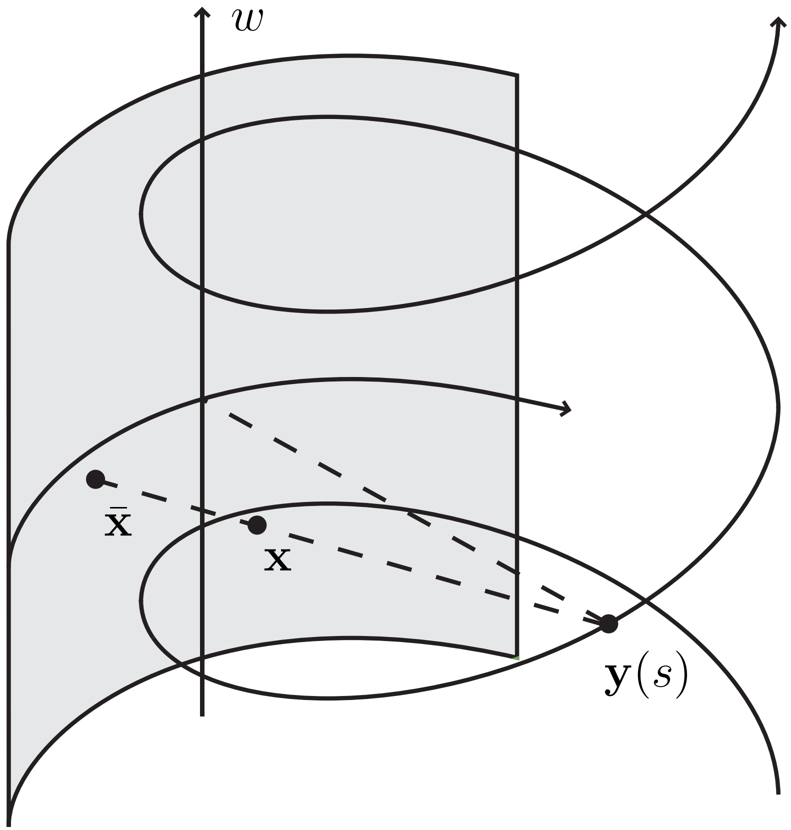

Which source positions are needed for reconstruction at a point $\mathbf{x}$?

π-line and π-interval

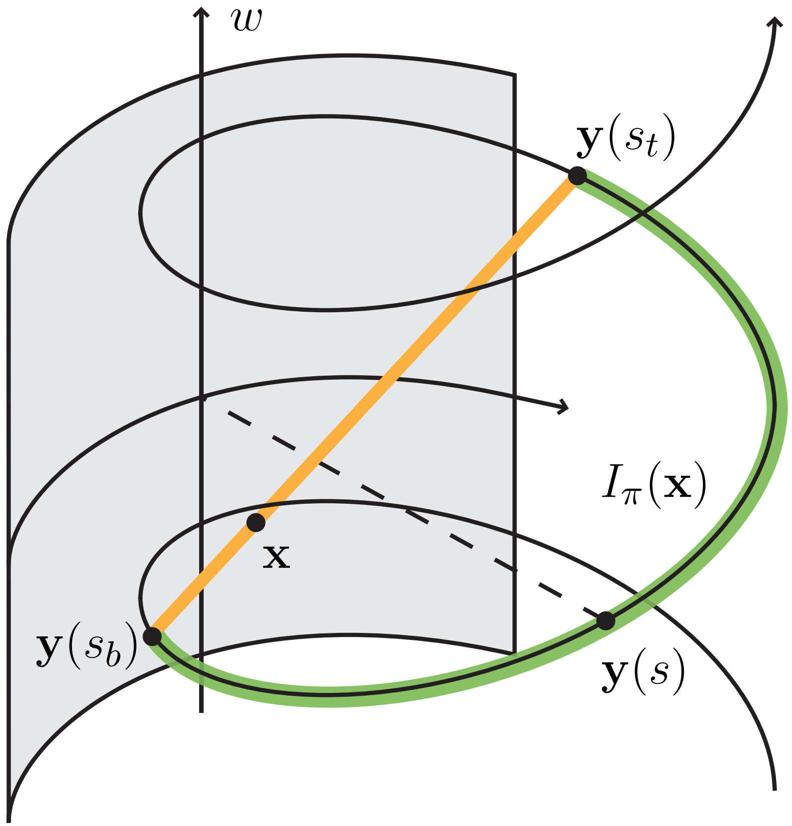

A so-called π-line through $\mathbf{x}$ intersects the source curve twice within one turn.

π-line and π-interval

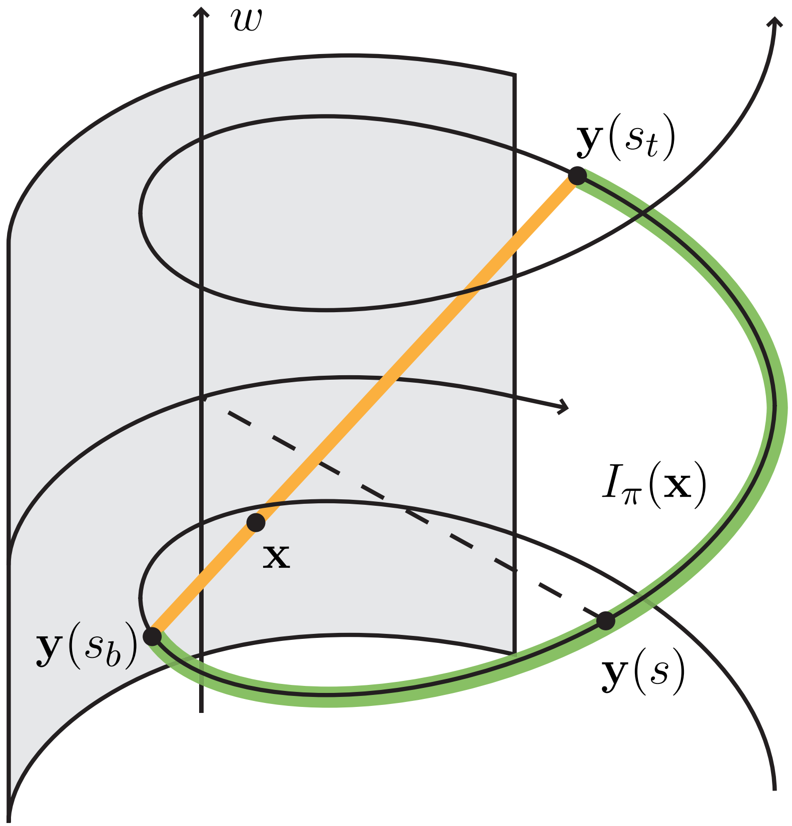

A so-called π-line through $\mathbf{x}$ intersects the source curve twice within one turn.
For the helix there is a unique π-line through $\mathbf{x}$.

π-line and π-interval

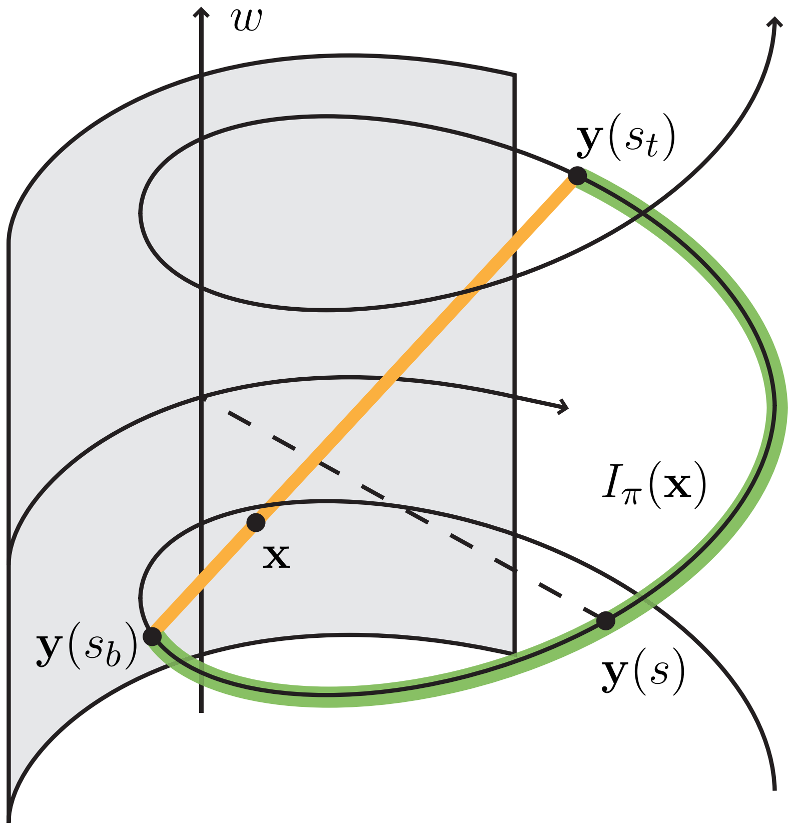

A π-line through $\mathbf{x}$ gives rise to the π-interval $I_\pi(\mathbf{x}) = [s_b(\mathbf{x}),\ s_t(\mathbf{x})]$.

π-line and π-interval

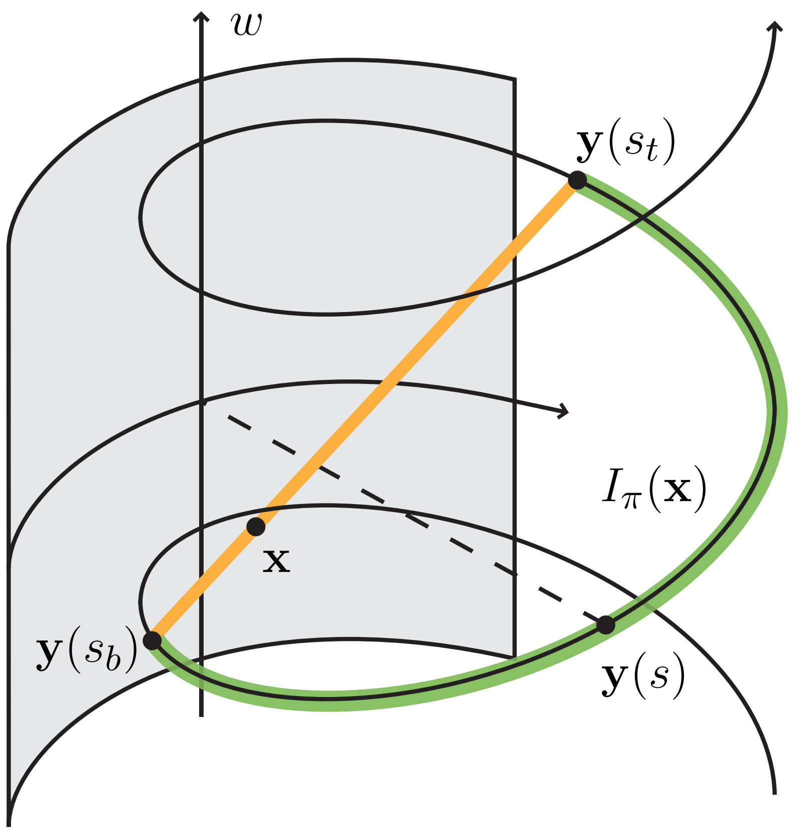

A π-line through $\mathbf{x}$ gives rise to the π-interval $I_\pi(\mathbf{x}) = [s_b(\mathbf{x}),\ s_t(\mathbf{x})]$.

Sources $\mathbf{y}(s)$ with $s \in I_\pi(\mathbf{x})$ lie on the green arc.

π-line reconstruction formulas

Definition 1 *A π-line reconstruction formula uses for reconstruction at a point $\mathbf{x}$ only data from sources within the π-interval of $\mathbf{x}$.*

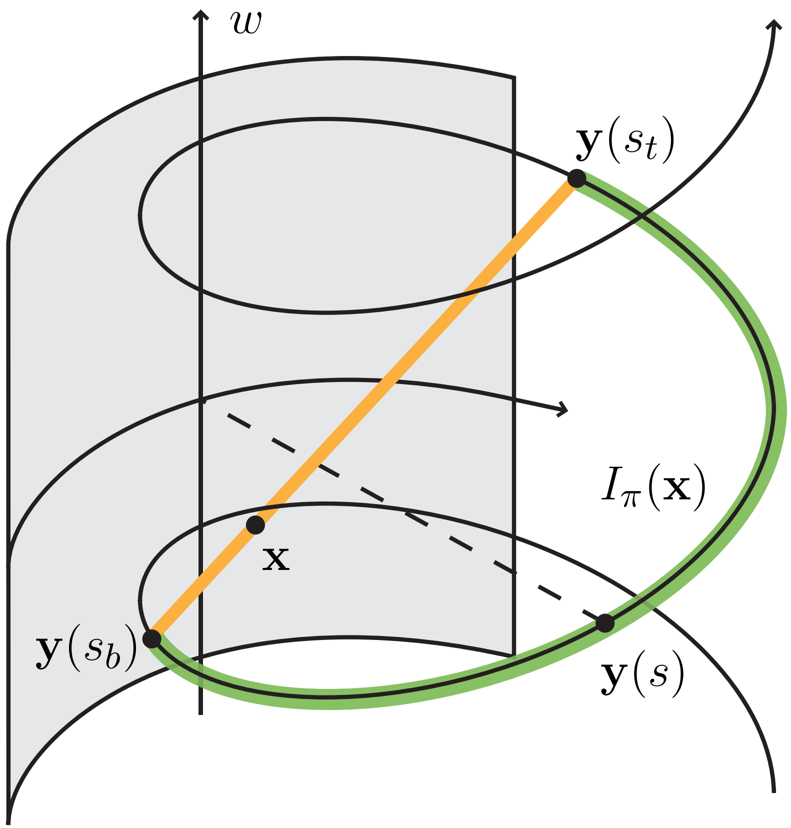

Example: Backprojection-filtration

Define the Hilbert transform of f in direction $\boldsymbol{\theta} \in S^{n-1}$ as

$$H_{\boldsymbol{\theta}} f(\mathbf{x}) = \frac{1}{\pi} \int_{\mathbf{R}} \frac{f(\mathbf{x} - t\boldsymbol{\theta})}{t} \, dt.$$

Then

$$\frac{-1}{2\pi} \int_{I_\pi(\mathbf{x})} \frac{1}{|\mathbf{x} - \mathbf{y}(s)|} \frac{\partial}{\partial q} \mathcal{D} f(\mathbf{y}(q), \boldsymbol{\beta}(s, \mathbf{x}))\Big|_{q=s} ds \; = \; H_{\boldsymbol{\beta}(s_b(\mathbf{x}), \mathbf{x})} f(\mathbf{x})$$

$\boldsymbol{\beta}(s, \mathbf{x}) =$ unit vector pointing from $\mathbf{y}(s)$ to $\mathbf{x}$.

Right-hand side is Hilbert transform along the π-line of $\mathbf{x}$.

Originally due to Gel’fand and Graev (1991). Basis for backprojection-filtration algorithm (Zou and Pan (2004)).

Example: Filtered backprojection

$$f(\mathbf{x}) = \frac{-1}{2\pi^2}\int_{I_\pi(\mathbf{x})} \frac{1}{|\mathbf{x}-\mathbf{y}(s)|}\int_0^{2\pi} \frac{\partial}{\partial q}\mathcal{D}f(\mathbf{y}(q),\boldsymbol{\Theta}(s,\mathbf{x},\gamma))\Big|_{q=s} \frac{d\gamma\, ds}{\sin\gamma}$$

$$\boldsymbol{\Theta}(s,\mathbf{x},\gamma) = \cos(\gamma)\boldsymbol{\beta}(s,\mathbf{x}) + \sin(\gamma)\boldsymbol{\beta}^\perp(s,\mathbf{x}).$$

$\boldsymbol{\beta}(s,\mathbf{x}) =$ unit vector pointing from $\mathbf{y}(s)$ to $\mathbf{x}$.

(Katsevich 02, 04, Katsevich & Kapralov 07)

Example: Filtered backprojection

$$f(\mathbf{x}) = \frac{-1}{2\pi^2} \int_{I_\pi(\mathbf{x})} \frac{1}{|\mathbf{x} - \mathbf{y}(s)|} \int_0^{2\pi} \frac{\partial}{\partial q} \mathcal{D}f(\mathbf{y}(q), \boldsymbol{\Theta}(s, \mathbf{x}, \gamma))\bigg|_{q=s} \frac{d\gamma\, ds}{\sin\gamma}$$

$$\boldsymbol{\Theta}(s, \mathbf{x}, \gamma) = \cos(\gamma)\boldsymbol{\beta}(s, \mathbf{x}) + \sin(\gamma)\boldsymbol{\beta}^\perp(s, \mathbf{x}).$$

$$\boldsymbol{\beta}(s, \mathbf{x}) = \text{ unit vector pointing from } \mathbf{y}(s) \text{ to } \mathbf{x}.$$

(Katsevich 02, 04, Katsevich & Kapralov 07)

Both formulas hold in dimensions 2 and 3 for a large family of source curves.

In dimension 3, $\boldsymbol{\beta}^\perp$ has to be carefully chosen (Katsevich 02, 04).

κ-Plane and Katsevich's formula

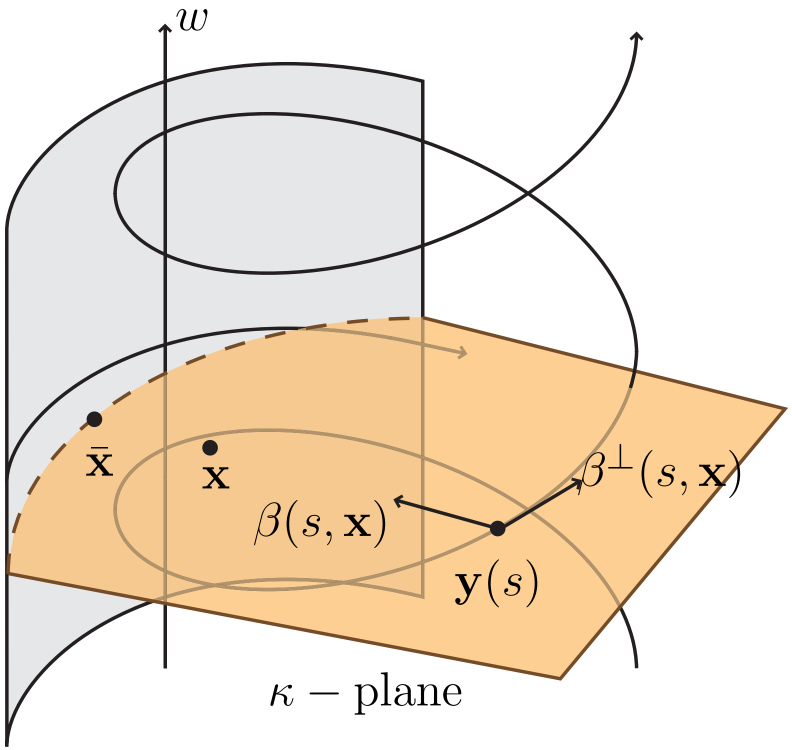

$$f(\mathbf{x}) = \frac{-1}{2\pi^2} \int_{I_\pi(\mathbf{x})} \frac{1}{|\mathbf{x}-\mathbf{y}(s)|} \int_0^{2\pi} \frac{\partial}{\partial q} \mathcal{D}f(\mathbf{y}(q), \boldsymbol{\Theta}(s,\mathbf{x},\gamma))\Big|_{q=s} \frac{d\gamma\, ds}{\sin\gamma}$$

$$\boldsymbol{\Theta}(s,\mathbf{x},\gamma) = \cos(\gamma)\boldsymbol{\beta}(s,\mathbf{x}) + \sin(\gamma)\boldsymbol{\beta}^{\perp}(s,\mathbf{x}).$$

Characteristics of π-line formulas

- Flexibility in choosing π-lines in 2D.

Non-uniqueness of π-lines in 2D

In 2 dimensions we lack uniqueness of π-lines. Any line through $\mathbf{x}$ may be chosen as the π-line of $\mathbf{x}$, denoted by $L_\pi(\mathbf{x})$.

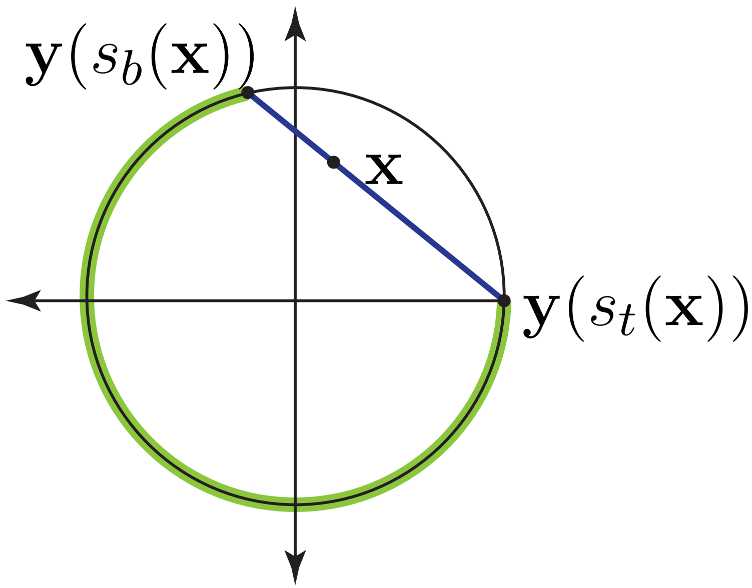

$I_\pi(\mathbf{x})$ may be chosen to correspond to either of the two arcs.

Example: Orthogonal-long π-lines

$L_\pi(\mathbf{x})$ is orthogonal to $\mathbf{x}$ and $I_\pi(\mathbf{x}) = [s_b(\mathbf{x}), s_t(\mathbf{x})]$ corresponds to the longer arc.

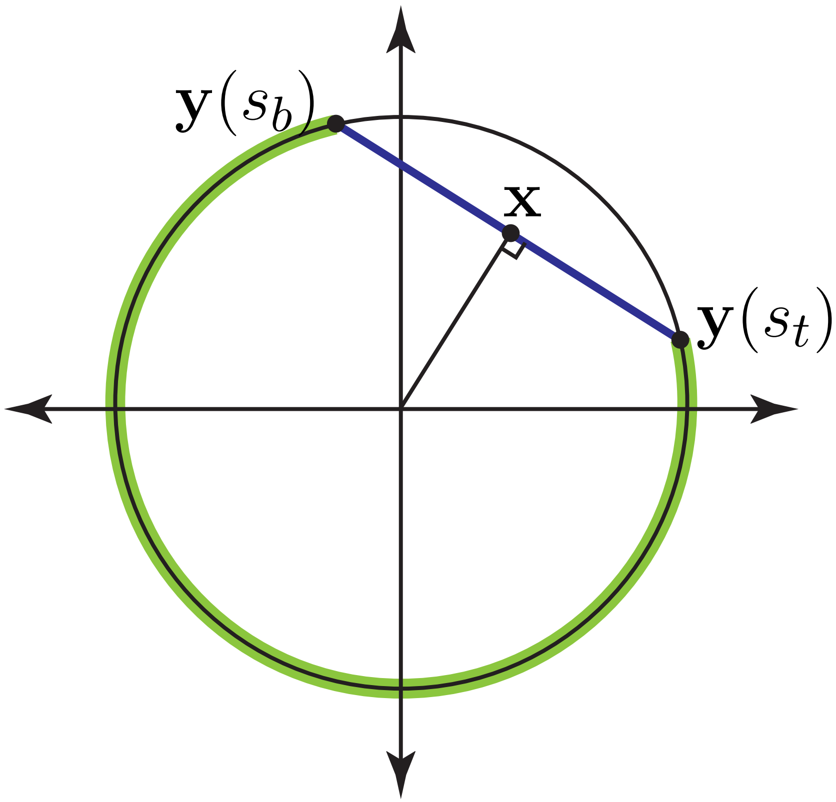

Superior performance for R close to 1!

Comparison for R=1.01

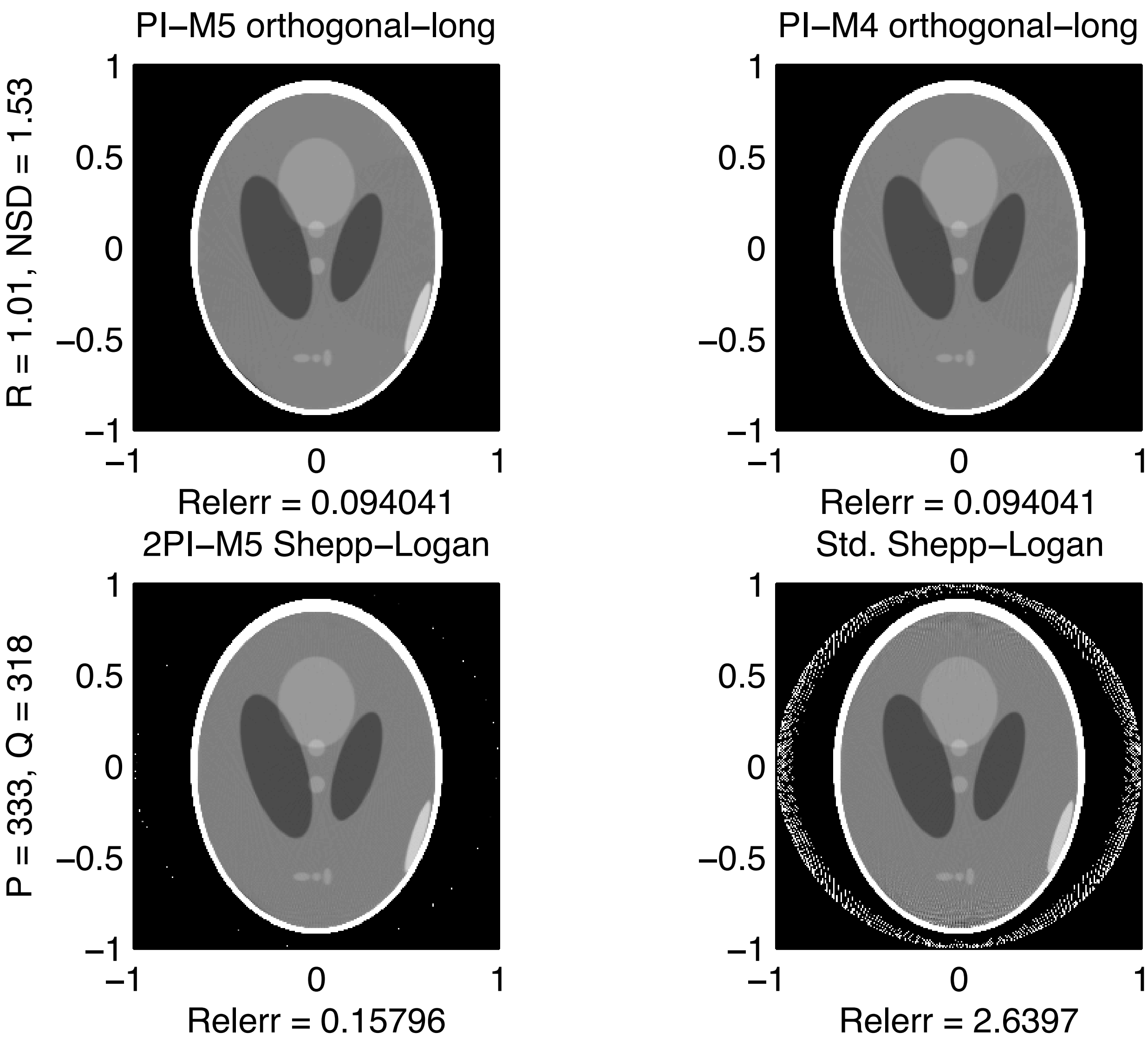

Characteristics of π-line formulas

- Flexibility in choosing π-lines in 2D.

Characteristics of π-line formulas

- Flexibility in choosing π-lines in 2D.
- Region of Backprojection not equal to S.
  RBP(s) $=$ set of all points where data from source $\mathbf{y}(s)$ is used for reconstruction $= \{\mathbf{x} : s \in I_\pi(\mathbf{x})\}$.
  RBP(s) depends on the family of π-lines.

Orthogonal-long π-lines

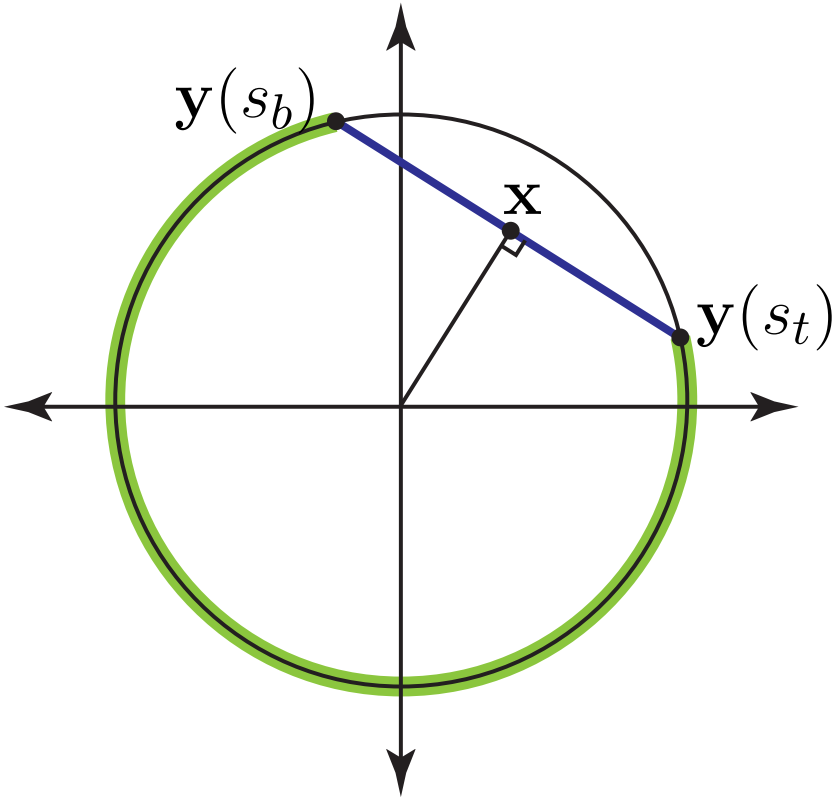

No two points have the same π-interval. The set $RBP(s)$ and its boundary are not immediately obvious.

RBP for orth.-long π-lines

For orthogonal-long π-lines, $RBP(s)$ contains all points outside the disk $D(s) = \{\mathbf{x} : |\mathbf{x} - \mathbf{y}(s)/2| < |\mathbf{y}(s)/2|\}$.

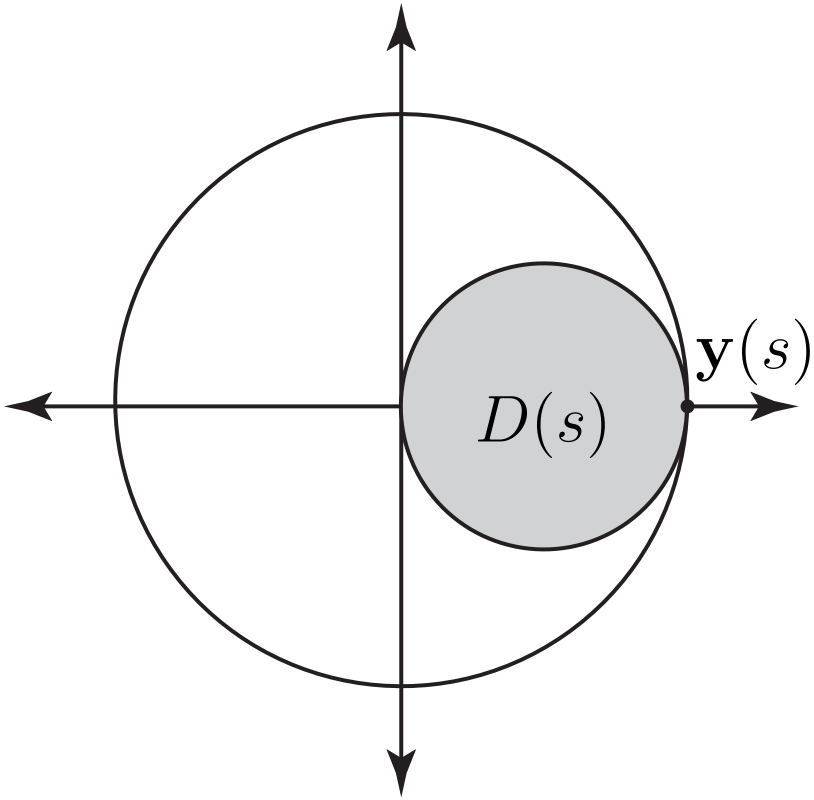

Hass-F., SIAM J. Imag Sci., (2012)

Sources close to object

The numerically most challenging parts of the reconstructions are those where data from an x-ray source contribute to the image at points very close to the source. But most of such points are not in the RBP for orthogonal long π-lines. So the most challenging parts are avoided!

Characteristics of π-line formulas

- Flexibility in choosing π-lines in 2D.

Characteristics of π-line formulas

- Flexibility in choosing π-lines in 2D.
- Region of Backprojection not equal to S.
  RBP$(s) =$ set of all points where data from source $\mathbf{y}(s)$ is used for reconstruction $= \{\mathbf{x} : s \in I_\pi(\mathbf{x})\}$.
  RBP(s) depends on the family of π-lines.

Characteristics of π-line formulas

- Flexibility in choosing π-lines in 2D.
- Region of Backprojection not equal to S.
  RBP$(s) =$ set of all points where data from source $\mathbf{y}(s)$ is used for reconstruction $= \{\mathbf{x} : s \in I_\pi(\mathbf{x})\}$.
  RBP(s) depends on the family of π-lines.
- Comet tail artifacts.

Comet tail artifacts

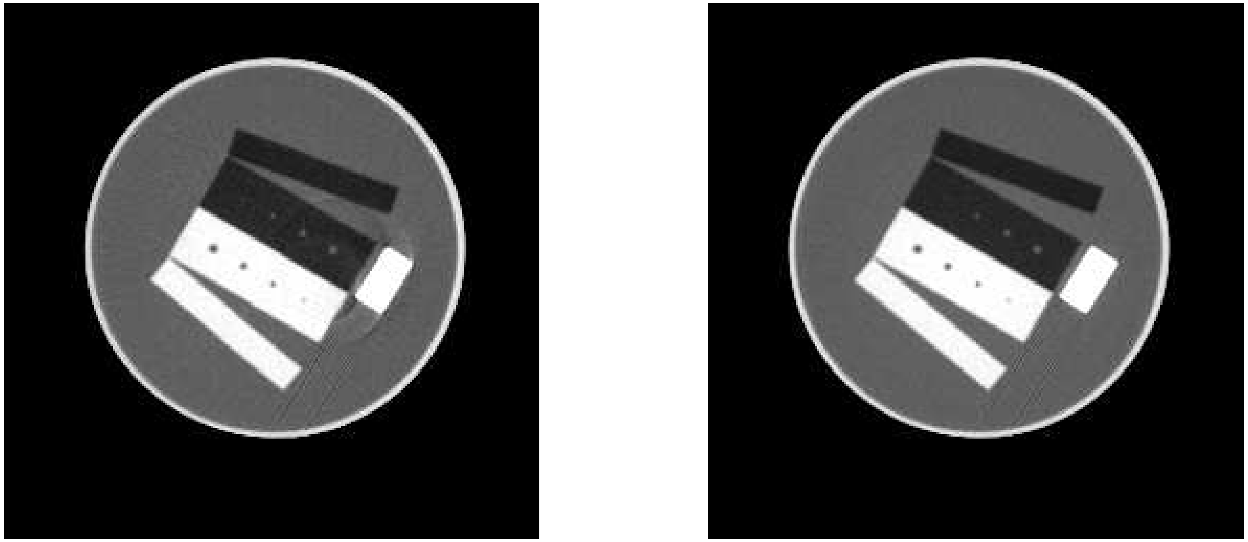

Reconstructions from real data. The reconstruction from the π-line filtered backprojection formula (left) shows a large comet tail artifact that is not present in a standard reconstruction (right).

Comet tail artifacts

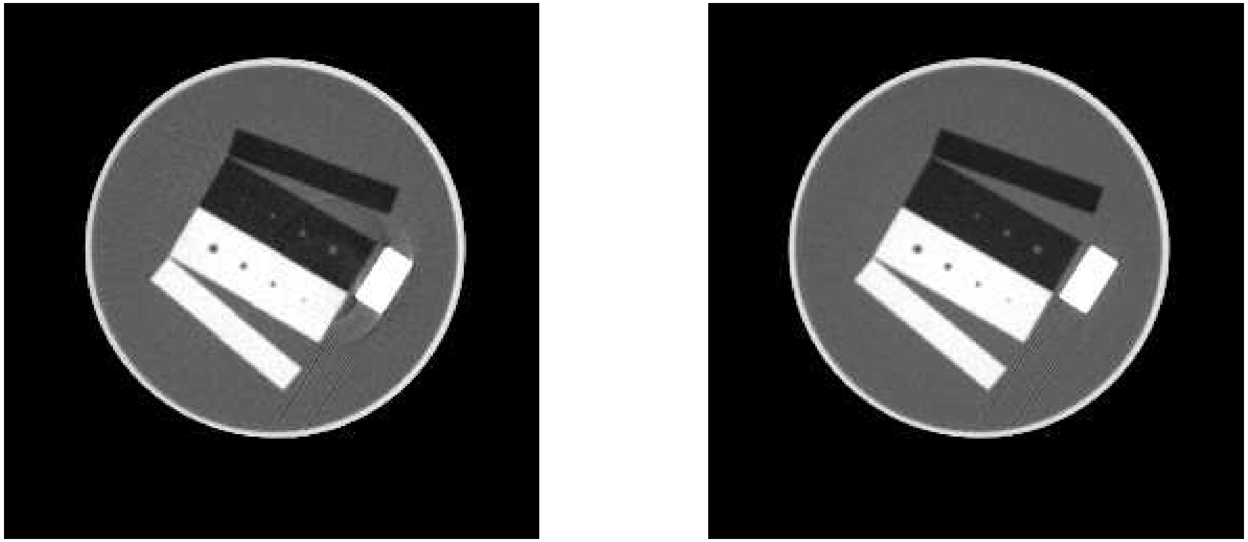

Reconstructions from real data. The reconstruction from the π-line filtered backprojection formula (left) shows a large comet tail artifact that is not present in a standard reconstruction (right).

In this case most of the artifact is due to a previously undetected data misalignment in the fan angle. The π-line formula is much more sensitive to such misalignments.

Finding the correct alignment

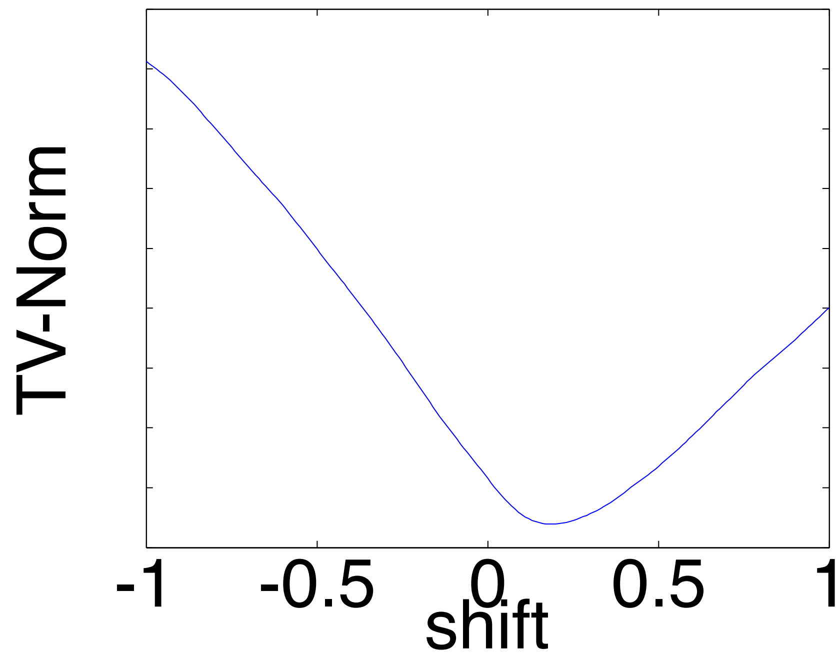

The correct alignment (about 0.19 detector widths) corresponds here to a minimum of the total variation $TV(f) = \int |\nabla f(\mathbf{x})| \, d\mathbf{x}$ (here of a subregion of the image).

Reconstruction with corrected alignment

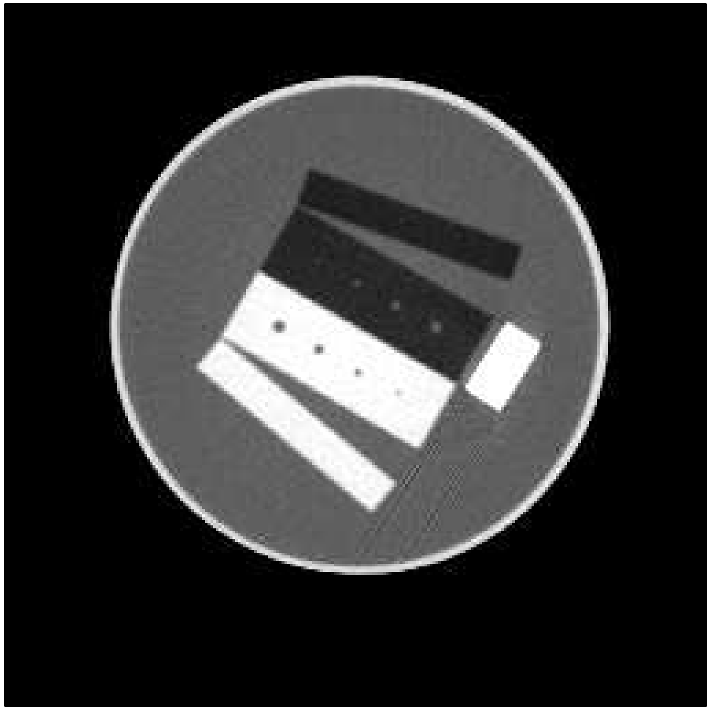

The comet tail artifact is much reduced.

Numerical implementation in 2D

The general FBP formula written in curved detector coordinates ($\gamma = \alpha^* - \alpha$):

$$f(\mathbf{x}) = \frac{-1}{2\pi^2} \int_{I_\pi(\mathbf{x})} \frac{1}{|\mathbf{x} - \mathbf{y}(s)|} \int_0^{2\pi} \frac{\partial}{\partial q} \mathcal{D}f(\mathbf{y}(q), \boldsymbol{\Theta}(s, \mathbf{x}, \gamma))\Big|_{q=s} \frac{d\gamma\, ds}{\sin\gamma}$$

$$= \frac{-1}{2\pi^2} \int_{I_\pi(\mathbf{x})} \frac{1}{|\mathbf{x} - \mathbf{y}(s)|} \int_0^{2\pi} \frac{\partial}{\partial q} \mathcal{D}f(\mathbf{y}(q), \boldsymbol{\Theta}(s, \alpha))\Big|_{q=s} \frac{d\alpha\, ds}{\sin(\alpha^* - \alpha)}$$

$$= \frac{1}{2\pi^2} \int_{I_\pi(\mathbf{x})} \frac{1}{|\mathbf{x} - \mathbf{y}(s)|} \int_0^{2\pi} \left(\frac{\partial g}{\partial s} + \frac{\partial g}{\partial \alpha} \right)(s, \alpha) \frac{d\alpha\, ds}{\sin(\alpha^* - \alpha)}$$

$\alpha^* = \alpha^*(s, \mathbf{x})$ corresponds to line through $\mathbf{y}(s)$ and $\mathbf{x}$.

Numerical implementation ...

Two discretizations need to be implemented carefully: The convolution with respect to α and the discretization of the view dependent derivative

$$\mathcal{D}f(\mathbf{y}(q),\mathbf{\Theta}(s,\alpha))\Big|_{q=s} = \left(\frac{\partial g}{\partial s} + \frac{\partial g}{\partial \alpha}\right)(s,\alpha) = g'(s,\alpha)$$

In this talk we focus on the latter. For the former, see F., Hass, Solmon (2008). Recall $g(s,\alpha) = Df(\mathbf{y}(s),\mathbf{\Theta}(s,\alpha))$.

Data measured for $(s_k,\alpha_l),\ s_k = k\Delta s,\ \alpha_l = l\Delta\alpha$.
Sampling theory: $\Delta s \geq (1+R)\Delta\alpha$.

Direct scheme.

Note: $\mathbf{\Theta}(s,\alpha) = \mathbf{\Theta}(s+u,\alpha+u)$.
Let $s_{k+\frac{1}{2}} = s_k + \Delta s/2$

$$g'(s_{k+\frac{1}{2}},\alpha_l) = \frac{\partial}{\partial q}\mathcal{D}f(\mathbf{y}(q),\mathbf{\Theta}(s_{k+\frac{1}{2}},\alpha_l))\Big|_{q=s_{k+\frac{1}{2}}}$$

$$\simeq \frac{1}{\Delta s}\Big(Df(\mathbf{y}(s_{k+1}),\mathbf{\Theta}(s_{k+\frac{1}{2}},\alpha_l)) - Df(\mathbf{y}(s_k),\mathbf{\Theta}(s_{k+\frac{1}{2}},\alpha_l))\Big)$$

$$= (\Delta s)^{-1}(g(s_{k+1},\alpha_l+\Delta s/2) - g(s_k,\alpha_l-\Delta s/2))$$

Use linear interpolation in α for $g(s_{k+1},\alpha_l+\Delta s/2)$, $g(s_k,\alpha_l-\Delta s/2)$.

Unified framework

Unified framework for comparison: Write all schemes as approximations for $\left(\frac{\partial g}{\partial s} + \frac{\partial g}{\partial \alpha}\right)(s, \alpha)$.

Direct scheme: $g'(s_{k+\frac{1}{2}}, \alpha_l) \simeq$

$$\frac{1}{2\Delta s}\left[g(s_{k+1}, \alpha_l + \Delta s/2) - g(s_k, \alpha_l + \Delta s/2)\right.$$

$$\left. + g(s_{k+1}, \alpha_l - \Delta s/2) - g(s_k, \alpha_l - \Delta s/2)\right]$$

$$+ \frac{1}{2\Delta s}\left[g(s_{k+1}, \alpha_l + \Delta s/2) - g(s_{k+1}, \alpha_l - \Delta s/2)\right.$$

$$\left. + g(s_k, \alpha_l + \Delta s/2) - g(s_k, \alpha_l - \Delta s/2)\right]$$

Stepsize $\Delta s >> \Delta\alpha$ too large in approximation of $\frac{\partial g}{\partial \alpha}$!

Noo-Pack-Heuscher (NPH) scheme ('03)

Let $g_{k,l} = g(s_k, \alpha_l)$, etc.

$$g'(s_{k+\frac{1}{2}}, \alpha_{l+\frac{1}{2}}) \simeq \frac{1}{2\Delta s}\left[(g_{k+1,l+1} - g_{k,l+1}) + (g_{k+1,l} - g_{k,l})\right]$$

$$+ \frac{1}{2\Delta\alpha}\left[(g_{k+1,l+1} - g_{k+1,l}) + (g_{k,l+1} - g_{k,l})\right]$$

Now $\frac{\partial g}{\partial \alpha}$ is approximated with stepsize $\Delta\alpha$. Much better results than direct scheme, but non-isotropic resolution!

Non-isotropic resolution of NPH

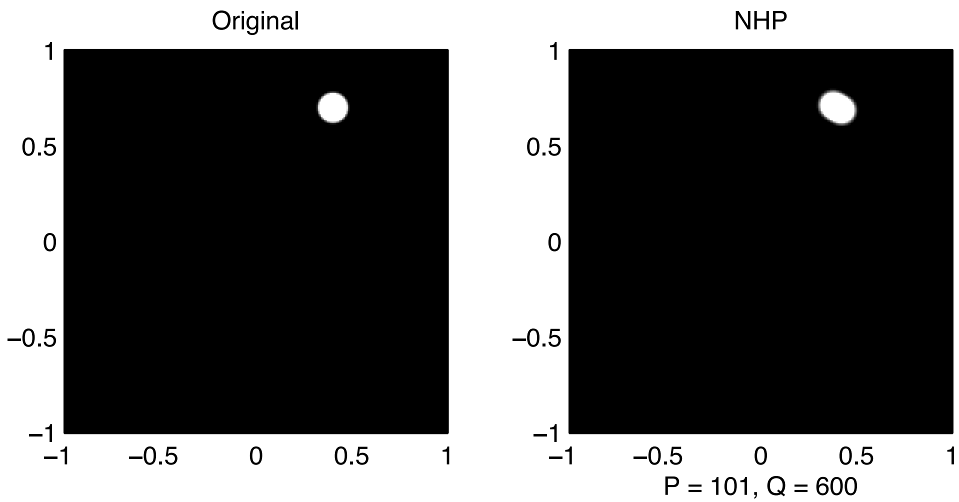

The radial resolution is better than the tangential resolution.

Noo et al (NHDLH) scheme ('07)

Let $0 < \epsilon \leq 1$ be a free parameter and $\mathbf{\Theta} = \mathbf{\Theta}(s_k, \alpha_{l+\frac{1}{2}})$.

$$g'(s_k, \alpha_{l+\frac{1}{2}}) \simeq \frac{Df(\mathbf{y}(s_k + \epsilon \Delta s), \mathbf{\Theta}) - Df(\mathbf{y}(s - \epsilon \Delta s), \mathbf{\Theta})}{2\epsilon \Delta s}$$

Interpolation needed. Approximate

$$Df(\mathbf{y}(s_k + \epsilon \Delta s), \mathbf{\Theta}) \simeq (1-\epsilon) g(s_k, \nu_+) + \epsilon g(s_{k+1}, \mu_+)$$

$$Df(\mathbf{y}(s_k - \epsilon \Delta s), \mathbf{\Theta}) \simeq (1-\epsilon) g(s_k, \nu_-) + \epsilon g(s_{k-1}, \mu_-)$$

and then use linear interpolation in α for the $g(s_k, \nu_+), \ldots$.
The $\nu_\pm, \mu_\pm$ come from the following diagram.

Interpolation step in NHDLH scheme

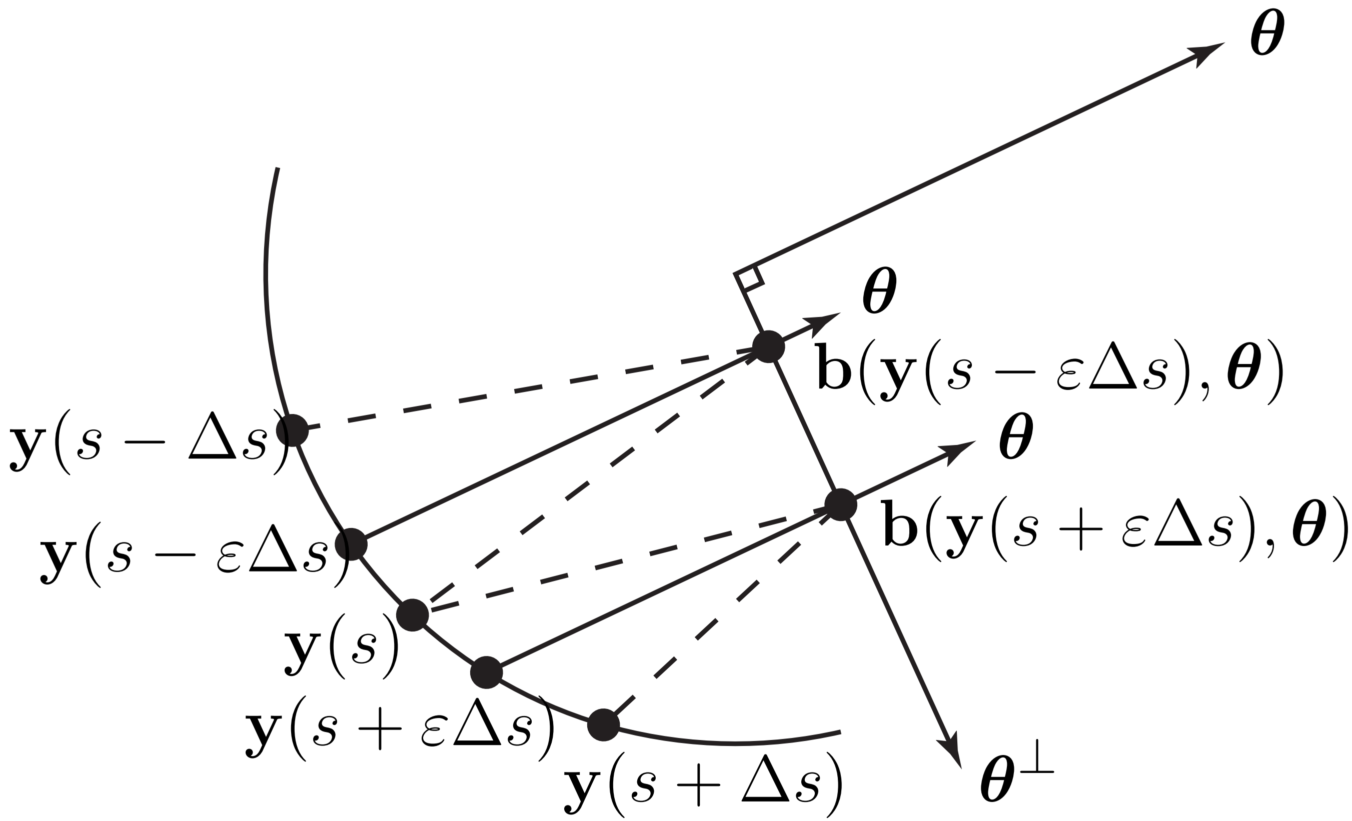

Figure 1: $\mathrm{b}(t,\boldsymbol{\Theta})=\mathbf{y}(t)-(\mathbf{y}(t)\cdot\boldsymbol{\Theta})\boldsymbol{\Theta}$. The dashed lines represent $g(s,\nu_{\pm}), g(s+\Delta s,\mu_{+}), g(s-\Delta s,\mu_{-})$.

NHDLH scheme in unified framework

Proposition 1 *Let ϵ be sufficiently small, such that all $\nu_\pm, \mu_\pm \in [\alpha_l, \alpha_{l+1}]$ and let $c = (\mu_+ - \alpha_l)/\Delta\alpha$. Then the NDHLH scheme reads :* $g'(s_k, \alpha_{l+\frac{1}{2}}) \simeq$

$$g'(s_k, \alpha_{l+\frac{1}{2}}) \simeq \left((1-c)\,\frac{g_{k+1,l} - g_{k-1,l}}{2\Delta s} + c\,\frac{g_{k+1,l+1} - g_{k-1,l+1}}{2\Delta s}\right)$$

$$+ \left((1-\epsilon)\,\frac{\nu_+ - \nu_-}{2\epsilon\Delta s}\,\frac{g_{k,l+1} - g_{k,l}}{\Delta\alpha} + \epsilon\,\frac{\mu_+ - \mu_-}{2\epsilon\Delta s}\,\frac{g_{k-1,l+1} - g_{k-1,l}}{\Delta\alpha}\right)$$

$$c = \frac{1}{2} + \epsilon\frac{\Delta s}{\Delta\alpha} + O(\Delta s \tan\alpha_l), \qquad \frac{\nu_+ - \nu_-}{2\epsilon\Delta s} = 1 + O((\epsilon\Delta s)^2)$$

$$\frac{\mu_+ - \mu_-}{2\epsilon\Delta s} = 1 + O\left((\sec\alpha_l(1-\epsilon)\Delta s)^2/\epsilon\right)$$

Is there a simpler way?

What is the cause of the non-isotropic resolution in NHP?

$$g'(s_{k+\frac{1}{2}}, \alpha_{l+\frac{1}{2}}) \simeq \frac{1}{2\Delta s}\left[(g_{k+1,l+1} - g_{k,l+1}) + (g_{k+1,l} - g_{k,l})\right]$$

$$+ \frac{1}{2\Delta \alpha}\left[(g_{k+1,l+1} - g_{k+1,l}) + (g_{k,l+1} - g_{k,l})\right]$$

Answer: The averaging in the derivative with respect to α. Each of the two parts by itself leads to a slightly rotated image.

Cause of NHP non-isotropy

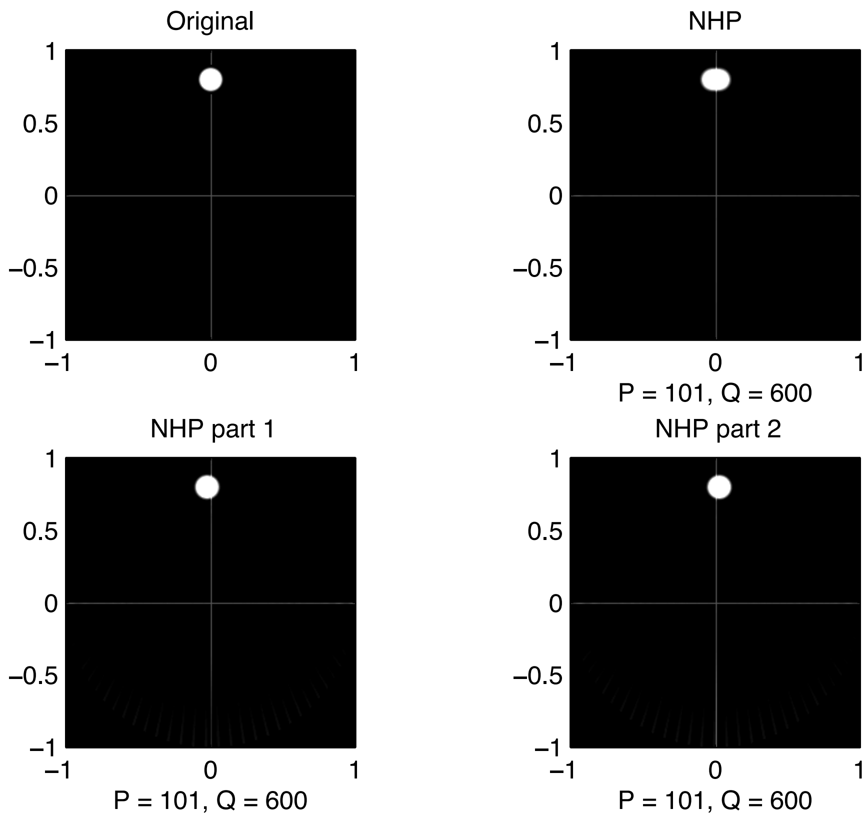

FHS scheme (F.-Hass-Solmon ('08))

$$g'(s_k, \alpha_{l+\frac{1}{2}}) \simeq \frac{\left(g_{k+1,l} - g_{k-1,l}\right) \ + \ \left(g_{k+1,l+1} - g_{k-1,l+1}\right)}{4\Delta s}$$

$$+ \quad \frac{g_{k,l+1} - g_{k,l}}{\Delta \alpha}$$

Removes the drawbacks of the NPH scheme, is simpler than NHDLH and performs on par with NHDLH for a circular source curve.

K scheme (Katsevich '11)

$$g'(s_k, \alpha_{l+\frac{1}{2}}) \simeq \epsilon \frac{(g_{k+1,l+1} - g_{k,l+1}) \ + \ (g_{k,l} - g_{k-1,l})}{2\Delta s}$$

$$+ (1-\epsilon)\frac{(g_{k+1,l} - g_{k,l}) + (g_{k,l+1} - g_{k-1,l+1})}{2\Delta s}$$

$$+ \ \frac{g_{k,l+1} - g_{k,l}}{\Delta \alpha}$$

Katsevich found $\epsilon = 1/2$ to be a good tradeoff between stability and accuracy. For $\epsilon = 1/2$ this scheme simplifies to the FHS scheme.

Leading error terms

FHS: $$(\Delta\alpha)^2\left(\frac{g_{\alpha\alpha\alpha}}{24}+\frac{g_{s\alpha\alpha}}{8}\right) + (\Delta s)^2\,\frac{g_{sss}}{6}$$

NPH: $$(\Delta\alpha)^2\left(\frac{g_{\alpha\alpha\alpha}}{24}+\frac{g_{s\alpha\alpha}}{8}\right) + (\Delta s)^2\,\left(\frac{1}{4}\frac{g_{sss}}{6} + \frac{g_{ss\alpha}}{8}\right)$$

K: $$(\Delta\alpha)^2\left(\frac{g_{\alpha\alpha\alpha}}{24}+\frac{g_{s\alpha\alpha}}{8}\right) + (\Delta s)^2\,\frac{g_{sss}}{6} + \Delta s\Delta\alpha(1-2\epsilon)\frac{g_{ss\alpha}}{4}$$

NHDLH: $$(\Delta\alpha)^2\left(\frac{g_{\alpha\alpha\alpha}}{24}+\frac{g_{s\alpha\alpha}}{8}\right) + (\Delta s)^2\,\frac{g_{sss}}{6}$$

$$+\,(\Delta s)^2\,\left(d(\epsilon,\alpha)g_\alpha - \frac{(1-\epsilon)^2}{2}\tan\alpha\, g_{s\alpha} + \frac{\epsilon}{2}g_{ss\alpha}\right)$$

$$d(\epsilon,\alpha) = O((1-\epsilon)^2\sec^2\alpha)$$

Effect of extra error term in NPH

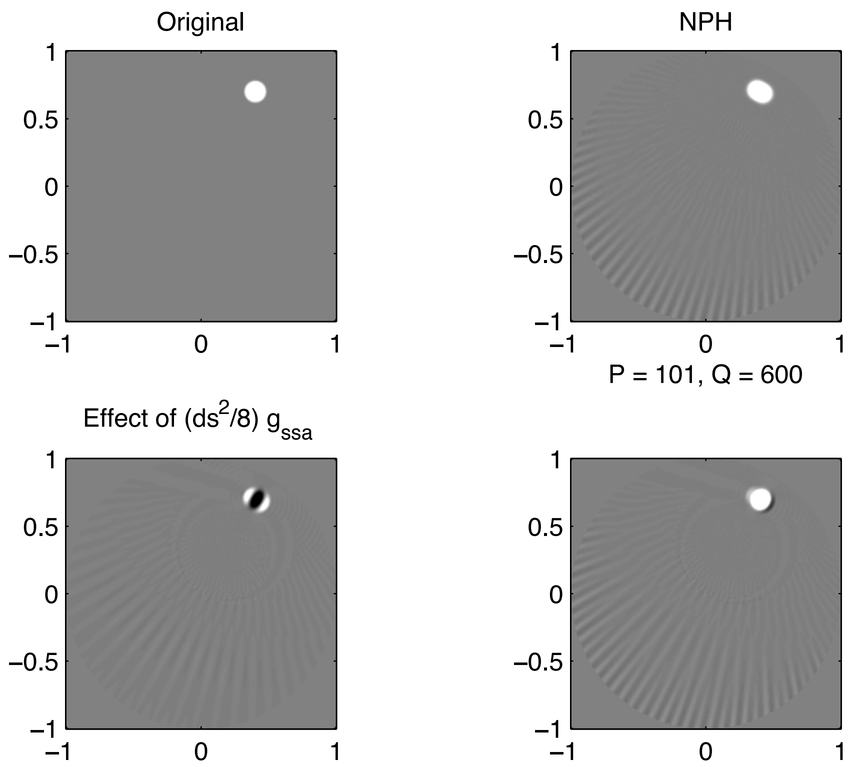

The extra term $(\Delta s)^2 \, \frac{g_{ss\alpha}}{8}$ appears to be largely responsible for the non-isotropic resolution.

Summary

- Error analysis consistent with numerical experience.
- FHS, K, and NHDLH perform equally well for a circular source curve.
- NHDLH has error terms that will become large for α very close to $\pi/2$. This can only occur when source is very close to object.
- Similar numerical results for elliptical source curve and curved detectors and flat detectors aligned perpendicular to $\mathbf{y}(s)$.
- However, for elliptical source curves NHDLH works also well for flat detectors aligned parallel to $\mathbf{y}'(s)$ while the analogues of the other methods do not (yet).

Some references

A. Faridani, R. Hass and D.C. Solmon, J. Phys. Conf. Ser., 124 (2008) 012024 (FHS)

R. Hass, and A. Faridani, SIAM J. Imag. Sci., 5 (2012), 1159–1184 (RBP, comet tail)

A. Katsevich, Adv. Appl. Math. 32(2004), 681–697

A. Katsevich and A. Kapralov, SIAM J. Appl. Math. 68(2007), 334–353

A. Katsevich, Phys. Med. Biol., 56 (2011), N53–N61 (K)

F. Noo et al., Phys. Med. Biol. 47(2002), 2525–2546

F. Noo, J. Pack, D. Heuscher, Phys. Med. Biol., 48 (2003), 3787 (NPH)

F. Noo et al, Phys. Med. Biol., 52 (2007), 5393–5414 (NHDLN)